

## Technical Paper

# Effects of different fine aggregates on the properties of ultra-high strength concrete

Taku Matsuda\* and Takafumi Noguchi

(Received: July 27, 2017; Accepted: November 29, 2017; Published online: January 5, 2018)

**Abstract:** When a coarse pore-structured fine aggregate with a large water absorption was used for concrete with a water-binder ratio of 0.12, unit water content of 135 kg/m<sup>3</sup>, and sand-aggregate ratio of 55%, the mobility, strength, and elastic modulus of concrete increased, with the autogenous shrinkage becoming extremely low. The authors attributed the reason for this phenomenon to the internal curing effect of fine aggregate based on tests using mortar samples and the properties of fine aggregate. The authors also considered that one reason for the increased strength of concrete is the reduction in the autogenous shrinkage of the mortar phase, which reduces the risk of failure under local stress, based on the stress-strain relationship of concrete and mortar under compressive deformation.

**Keywords:** ultra-high-strength concrete, fine aggregate, internal curing, pore structure.

## 1. Introduction

In their earlier study [1,2], the authors investigated the effect of using silica fume and fly ash in combination as supplementary cementitious materials (SCMs) for ultrahigh strength concrete with a water-binder ratio (W/B) of 0.20 or less. As a result, concrete made using both SCMs, silica fume and fly ash, led to a lower viscosity than with silica fume alone. Therefore, sufficient mobility was achieved even by reducing the unit water content (W) from 150 kg/m<sup>3</sup> to 135 kg/m<sup>3</sup> and increasing the sand-aggregate ratio (s/a) from 27% to 55%. The strength and elastic modulus thus increased and the autogenous shrinkage significantly decreased. (Figure 1 shows part of the results of the study [2]). However, these are results of tests conducted using specific materials (low-heat portland cement, silica fume, fly ash, ferronickel slag fine aggregate, and crushed hard sandstone). The purpose of the present study is to examine the applicability of the above-mentioned results to ultrahigh strength concrete made using different materials, while considering the reason why different materials lead to different properties of concrete (mobility, mechanical proper-

ties, and autogenous shrinkage), thereby acquiring knowledge that contributes to the development of proportioning techniques.

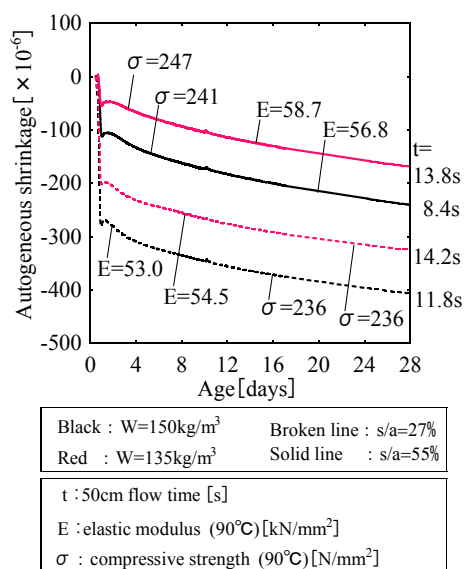


Fig. 1 – Part of the results of the early study [2]

Table 1 gives the materials used in the present tests, which were conducted in two series. The binders are premixed cement (SFPC) made by replacing a part of low-heat-type cement with silica fume, and fly ash (FA) conforming to Type I specified in JIS A 6201; the fine aggregates are andesite (S1), hard sandstone (S2), and two types of ferronickel slags (S3 and S4); the coarse aggregates are andesite (G1) and two types of hard sandstone (G2 and G3). G2 and G3 from different sources are

**Corresponding author Taku Matsuda** is the Chief of the Construction Material Group of the Technical Research Institute Technical & Engineering Service Division, Sumitomo Mitsui Construction Co., Ltd, Japan.

**Takafumi Noguchi** is a Prof. of the Dept. of Architecture, Graduate School of Eng., The University of Tokyo, Japan.

Table 1 – Materials

	Type	Characteristics	Symbol	Test series
B	Silica fume premixed cement	Density: 3.04g/cm <sup>3</sup> , Specific surface area: 5780cm <sup>2</sup> /g	SFPC	1, 2
	Fly ash	Density: 2.40g/cm <sup>3</sup> , Specific surface area: 5300cm <sup>2</sup> /g	FA	
S	Andensite	Density: 2.61g/cm <sup>3</sup> , Absorption: 2.81%	S1	
	Hard sandstone	Density: 2.61g/cm <sup>3</sup> , Absorption: 1.24%	S2	
	Ferronickel slag	Density: 2.89g/cm <sup>3</sup> , Absorption: 2.91%	S3	1, 2, earlier study [1,2]
		Density: 2.97g/cm <sup>3</sup> , Absorption: 0.95%	S4	2
G	Andensite	Density: 2.60g/cm <sup>3</sup> , Absorption: 2.48%	G1	1
	Hard sandstone (G <sub>max</sub> : 20mm)	Density: 2.64g/cm <sup>3</sup> , Absorption: 0.82%	G2	
	Hard sandstone (G <sub>max</sub> : 13mm)	Density: 2.63g/cm <sup>3</sup> , Absorption: 0.95%	G3	
SP	Chemical admixture	Polycarboxylate-based	SP	1, 2, earlier study [1,2]

Table 2 – Mix proportions (series 1)

Symbol	S	G	W/B	s/a [%]	Air [%]	Unit weight [kg/m <sup>3</sup> ]									Vs/ V <sub>mor</sub> **	Vs/ V <sub>paste</sub> **			
						W	B		S			G							
							SFPC	FA	S1	S2	S3	G1	G2	G3					
Con-1	S1 mixtures	S1	G1	0.12	29	1.5 +1.5, -1.0	155	1292	-	307	-	-	748	-	-	0.17	0.20		
Con-2	S2 mixtures	S2	G2						-	-	307	-	-	759	-				
Con-3	S1 mixtures	S1	G1					1034	258	287	-	-	709	-	-			0.15	0.18
Con-4	S2 mixtures	S2	G2				135	900	225	-	287	-	-	719	-	0.32	0.47		
Con-5		S2	G2							-	659	-	-	548	-				
Con-6	S3 mixtures	S3	G2							-	-	724	-	549	-			-	0.35
Con-7		S3	G3				-	-	724	-	-	547							
Con-8		S3	G3				125	834	208	-	-	786	-	-	592				
Con-9	S3	G3	48				95	634	158	-	-	845	-	-	850	0.43	0.76		

\*\*Vs/V<sub>mor</sub>: Volume ratio of fine aggregate to mortar\*\*\*Vs/V<sub>paste</sub>: Volume ratio of fine aggregate to paste

Table 3 – Types of specimens (series 1)

Curing condition		Test case	Specimen size [mm]	Test age [day]	Remark
20°C	20°C	Compressive strength	φ100×200 (Cylinder)	28	-
		Elastic modulus		28	-
		Compressive strength	φ50×100 (Cylinder)	28	Wet-screened mortar
		Elastic modulus		28	
		Autogeneous shrinkage	□100×100×400 (Prism)	28	-
90°C	20°C (48hr) ⇒ 90°C (120hr)	Compressive strength	φ100×200 (Cylinder)	7	-
		Elastic modulus		7	-
		Compressive strength	φ50×100 (Cylinder)	7	Wet-screened mortar
		Elastic modulus		7	

20 and 13 mm in maximum size, respectively. S3 and G3 are the same aggregates used in the earlier study [1,2]. In the present study, all specimens were seal-cured to eliminate the supply and escape of water.

## 2. Series 1

### 2.1 Test procedure and measurement items

Tables 2 and 3 give the mixture proportions of concrete and the types and curing conditions of

specimens, respectively. The W/B of all mixtures is fixed to 0.12. Con-1 and Con-2 in Table 2 represents mixtures containing silica fume but no fly ash, whereas Con-3 to Con-9 represent mixtures containing both silica fume and fly ash. Con-1 to Con-4 are proportioned with  $W = 155 \text{ kg/m}^3$  and  $s/a = 29\%$ ; Con-5 to Con-7, with  $W = 135 \text{ kg/m}^3$  and  $s/a = 55\%$ ; and Con-8 and Con-9 contain  $W = 125$  and  $95 \text{ kg/m}^3$ , respectively. In series 1, mixtures are distinguished by the type of fine aggregate.

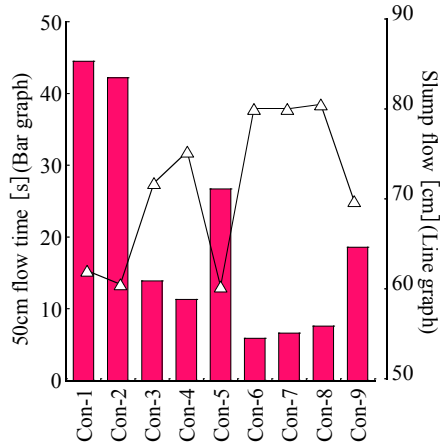


Fig. 2 – Slump flow (series 1)

Mixtures containing S1 as fine aggregate, for instance, are referred to as S1 mixtures for convenience sake, where appropriate. Wet-screened mortar was taken from each concrete mixture and cured under the same conditions as concrete. A twin-shaft forced-action mixer was used for mixing concrete, with the chemical admixture (SP) being added at the same dosage for all mixtures ( $B \times 2.30\%$ ). The air content and temperature of fresh concrete ranged from 2.0 to 3.0% and 28.5 to 32.0°C, respectively. The autogenous shrinkage was measured by strain transducers embedded in beams measuring  $100 \times 100 \times 400$  mm.

## 2.2 Test results and discussion

Figures 2 through 4, and Figure 6 show the results of slump flow tests, compression tests, elastic modulus tests, and autogenous shrinkage tests, respectively. Before going into the details, the results of Con-4 and Con-5 with fine aggregate S2 and coarse aggregate G2 are compared in these figures. A reduction in  $W$  from 155 to 135  $\text{kg}/\text{m}^3$  and an increase in  $s/a$  from 29 to 55% result in a reduction in the mobility but no marked changes in the strength, elastic modulus, and autogenous shrinkage. This is totally different from the tendencies of the earlier reports (Fig. 1) [2]. In other words, the properties of ultrahigh strength concrete can widely vary depending on the materials.

### 2.2.1 Mobility

As to the slump flow test results (see Fig. 2), the results of Con-1 to Con-4 demonstrate that the mobility of specimens containing both silica fume and fly ash is higher than that of specimens containing silica fume but no fly ash. No marked difference in mobility is observed between the aggregate combinations of S1 + G1 and S2 + G2 (between Con-1

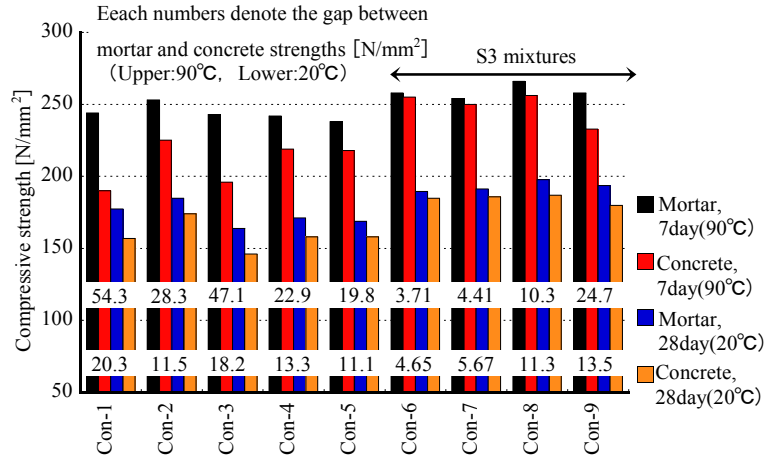


Fig. 3 – Compressive strength (series 1)

and -2 and between Con-3 and -4), as well as between coarse aggregates G2 and G3 (between Con-6 and -7). On the other hand, replacing S2 with S3 significantly reduces the viscosity (Con-5 to Con-6), resulting in concretes with viscosities lower than Con-1 and Con-2 even with a  $W$  of as low as 95  $\text{kg}/\text{m}^3$ . This is presumably because the mobility of the mortar phase of the S3 mixtures is higher than that of the other mixtures (This is to be verified using mortar samples later in Section 3 of this paper).

### 2.2.2 Mechanical properties

In the compression test results (see Fig. 3), as for S1 mixtures, the strength of Con-3 with combined SCMs of silica fume and fly ash is equivalent to those of specimens with a single SCM of silica fume (Con-1) after heating to 90°C, though the strength of the former is lower than the latter when kept at 20°C, similarly to the results of the earlier report [1]. Also, as for S2 mixtures, roughly same tendency also holds for the relationship between Con - 2 and Con - 4.

The mortar strength of all mixtures is higher than the concrete strength. In regard to Con-3 to Con-9 made using the same binder, both the concrete and mortar strengths are S1  $\approx$  S2 < S3 mixtures when these are kept at 20°C. After heating to 90°C, the mortar strength of all mixtures exceeds 240  $\text{N}/\text{mm}^2$ , with the comparison being S1  $\approx$  S2 < S3 mixtures. However, the concrete strength is S1 < S2 < S3 mixtures, with the gap between the mortar and concrete strengths of S1 mixtures being particularly wide (The reason for this is discussed at the end of this section and in Section 3).

Accordingly, one reason for the high concrete strength of S3 mixtures compared with those of S1 and S2 mixtures is the high strength of its mortar phase.

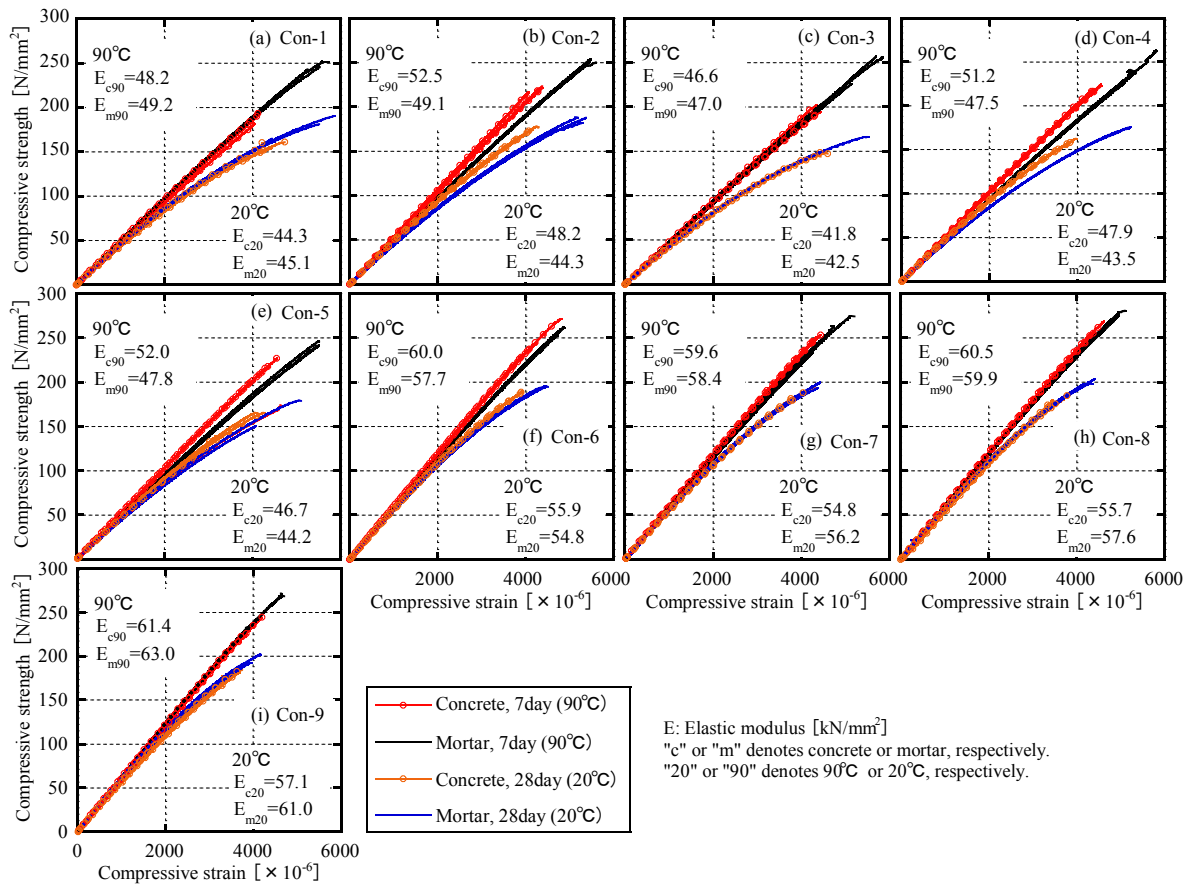


Fig. 4 – Elastic moduli of concrete and mortar specimens (series 1)

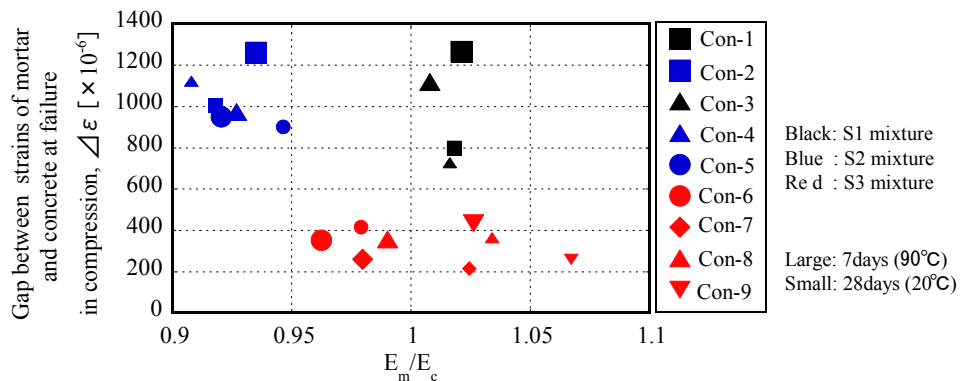


Fig. 5 – Relationship between the gap between the strains of mortar and concrete at failure in compression,  $\Delta\epsilon$  [ $\times 10^{-6}$ ], and the elastic modulus ratio ( $E_m/E_c$ )

As seen from Fig. 4, the elastic moduli of concrete and mortar specimens Con-3 to Con-9, which are made using the same binder components, are both in the order of S1 < S2 < S3 mixtures. The gradients of the stress-strain curves of concrete and mortar are nearly the same for S1 and S3 mixtures, whereas the gradient of the concrete curve for S2 is steeper than that of the mortar curve. Also, the compressive strain at break of each mortar specimen is greater than that of the corresponding con-

crete specimen.

Figure 5 shows the relationship between the gap between the strains of mortar and concrete at failure in compression,  $\Delta\epsilon$  [ $\times 10^{-6}$ ] (average of three specimens), and the elastic modulus ratio ( $E_m/E_c$ ). The  $\Delta\epsilon$  of S3 mixtures is evidently smaller than those of S1 and S2 mixtures.

The stiffnesses of hard sandstone G2 and G3 are assumed to be the same here, since no marked difference is observed between the results of Con-6

and Con-7 in which the proportioning conditions excepting coarse aggregate are the same. Based on this assumption, the mechanical properties of these mixtures are discussed. To begin with, S2 and S3 mixtures containing coarse aggregates with the same stiffnesses are examined. The stiffness of concrete falls between those of mortar and coarse aggregate, and the closer the stiffnesses of mortar and coarse aggregate, the closer the stiffnesses of concrete and mortar becomes. This suggests that the stiffness of the mortar phase of S3 mixtures is closer to those of coarse aggregate (G2 and G3) than that of S2 mixtures. According to the literature, the elastic modulus of hard sandstone (G2 and G3) falls in the range of 56.5 to 71.0 kN/mm<sup>2</sup> [3,4]). Based on this and the values in Fig. 4, the elastic moduli are roughly ranked as [the mortar phase of S2 mixtures < the mortar phase of S3 mixtures ≤ coarse aggregate (hard sandstone)]. The present discussion is thus considered to be valid. The stress distribution in the concretes of S3 mixtures under compressive loading is therefore more uniform than that in S2 mixtures. It follows that the former's concretes are less prone to failure under stress concentration due to the gap between the stiffnesses of coarse aggregate and mortar [5,6]. In other words,  $E_m/E_c$  of S3 mixtures is closer to 1.0 than that of S2 mixtures, with  $\Delta\epsilon$  being smaller (see Fig. 5). This explains the fracture strength of S3 mixtures being higher than that of S2 mixtures (see Fig. 3).

As for S1 mixtures, the stress-strain curves of concrete are shaped similarly to those of mortar (Fig. 4), with their  $E_m/E_c$  distributing closer to 1.0 than those of S3 mixtures (Fig. 5). However,  $\Delta\epsilon$  of S1 mixtures is evidently greater than that of S3 mixtures. According to the literature, the strength of andesite, the coarse aggregate of S1 mixtures, falls in the range of 182 to 218 N/mm<sup>2</sup> [3,4,7]. The concrete strengths of S1 mixtures heated to 90°C and those kept at 20°C are 190 to 196 N/mm<sup>2</sup> and 146 to 157 N/mm<sup>2</sup>, respectively. Therefore, there is a possibility that the large  $\Delta\epsilon$  of concrete heated to 90°C is due to the coarse aggregate failure before mortar failure. However,  $\Delta\epsilon$  of concrete kept at 20°C is greater than that of S3 mixtures, despite the fact that the strength of concrete kept at 20°C is lower than that of concrete heated to 90°C and therefore less prone to aggregate failure. This demonstrates the presence of a factor that determines the compressive strength of concrete other than the strength and stiffness of coarse aggregate and the mortar phase (This factor is discussed in section 3).

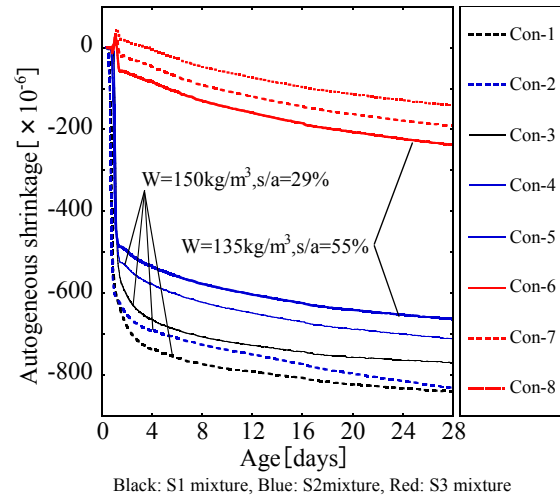


Fig. 6 – Autogenous shrinkage (series 1)

### 2.2.3 Autogenous shrinkage

According to the results of autogenous shrinkage tests (Fig. 6), the autogenous shrinkage of mixtures containing SCMs of silica fume and fly ash (Con-3 and Con-4) is smaller than that of mixtures solely containing silica fume as a SCM (Con-1 and Con-2). Also, when comparing among mixtures in which the proportioning conditions are the same excepting fine aggregate, the autogenous shrinkages are found to be S2 mixtures < S1 mixtures from Con-1 to Con-2, and from Con-3 to Con-4. It is also found from Con-5 to Con-6 that the autogenous shrinkages are S3 mixtures < S2 mixtures. Since the autogenous shrinkage of Con-6 is significantly smaller than that of Con-5, the autogenous shrinkage of the mortar phase of S3 mixtures is considered to be extremely small (The reason for this is discussed in section 3).

Based on the discussion regarding series 1, it can be said that the strongest impact on the properties of concrete is brought about by the difference of fine aggregate.

## 3. Series 2

Series 2 ascertains the differences in the mortar properties due to differences of fine aggregate by testing and discusses (1) the effect of the differences in the mortar properties on the concrete properties and (2) the reason why the differences of fine aggregate cause differences in the mortar properties.

### 3.1 Test procedure and measurement items

In addition to fine aggregates S1 to S3, ferrous slag S4 was included in the investigation. The saturated surface dry (SSD) density of S1 and S2 is the same, but the water absorption of S1 is greater than that of S2. As for ferrous slags S3 and S4, their SSD densities are the same, but the

Table 4 – Mix proportions (series 2)

Symbol	S	W/B	Air [%]	Unit weight [kg/m <sup>3</sup> ]			V <sub>s</sub> /V <sub>mor</sub> ※	V <sub>s</sub> /V <sub>paste</sub> ※※	SP [B*%]	Properties of fresh mortar				
				W	B					S	Air [%]	Temp. [°C]	0-impact flow ※※※[mm]	JP funnel flow [s]
					SFPC	FA								
S-1	S1	0.18	3.0 ±2.0	180	800	200	0.44	0.80	1.40	2.5	26.8	278	131	
S-2	S2									2.6	25.6	250	147	
S-3	S3									2.0	25.5	330	66	
S-4	S4									1.3	25.6	345	54	

※V<sub>s</sub>/V<sub>mor</sub>: Volume ratio of fine aggregate to mortar ※※V<sub>s</sub>/V<sub>paste</sub>: Volume ratio of fine aggregate to paste ※※※JIS R 5201

Table 5 – Types of specimens (series 2)

Curing condition	Test case	Specimen size [mm]	Test age [day]
20°C	Compressive strength	φ50×100 (Cylinder)	4, 7, 28
	Elastic modulus		28
	Autogenous shrinkage	□100×100×400 (Prism)	28
	Uniaxial restraining stress	□100×100×850 (Prism)	28
90°C	Compressive strength	φ50×100(Cylinder)	7
	Elastic modulus		7

water absorption of S3 is greater than that of S4. As for andesite S1 and ferronickel slag S3, their water absorptions are similar, but the SSD density of S3 is greater than that of S1. Tables 4 and 5 give the mixture proportions and fresh properties of mortar and the types and curing conditions of specimens, respectively. The W/B and V<sub>s</sub>/V<sub>mor</sub> are 0.18 and 0.44, respectively, to increase the W/B from the value for Series 1 (W/B = 0.12, V<sub>s</sub>/V<sub>mor</sub> = 0.17 to 0.43) to reduce the viscosity of the paste, while increasing the fine aggregate content, in expectation of emphasizing the effect of fine aggregate on the properties of mortar. A paddle mixer was used for mixing, with the dosage of SP being fixed (B × 1.40%) for all mixtures. In the autogenous shrinkage testing, uniaxial restraining tests using D10 deformed bars were conducted similarly to an earlier report [8]. Samples cured under the same conditions as strength test specimens were pulverized at the time of strength testing and dried at 105°C to measure the amount of evaporating water. The pore size distribution was also measured by mercury intrusion.

3.2 Test results and discussion

3.2.1 Mobility

The mobility of mortar made using S3 or S4 (S-3 and S-4) is found to be higher than that of mortar made using S1 or S2 (S-1 and S-2), as the 0-impact flow of the former is larger and the JP funnel flow through time of the former is shorter (The mobility of concrete made using this mortar is therefore greater as shown in Table 4).

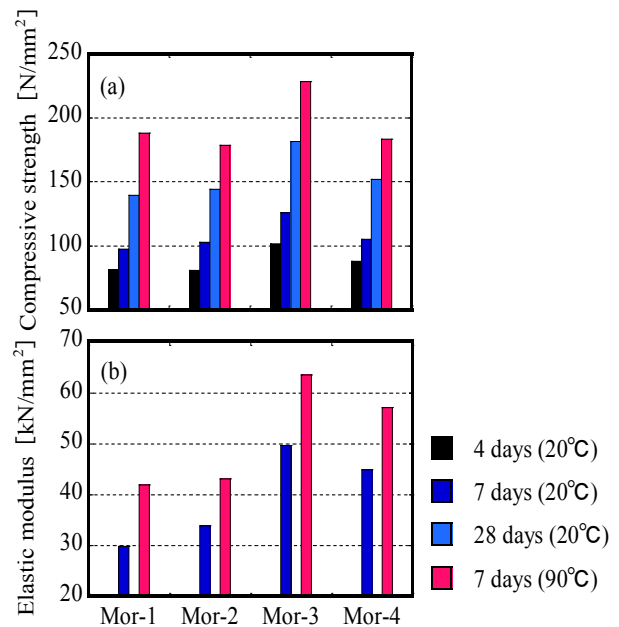


Fig. 7 – Compressive strength and elastic modulus (series 2)

3.2.2 Mechanical properties

The compressive strengths are S-1 ≈ S-2 ≈ S-4 < S-3, regardless of the curing conditions. The elastic moduli of S-3 and S-4 are higher, regardless of the curing conditions (see Fig. 7). The high strength and elastic modulus tendencies of S-3 are analogous to mortars in series 1.

3.2.3 Autogenous shrinkage

Figure 8 shows the results of autogenous shrinkage tests. The results until an age of 2 days,

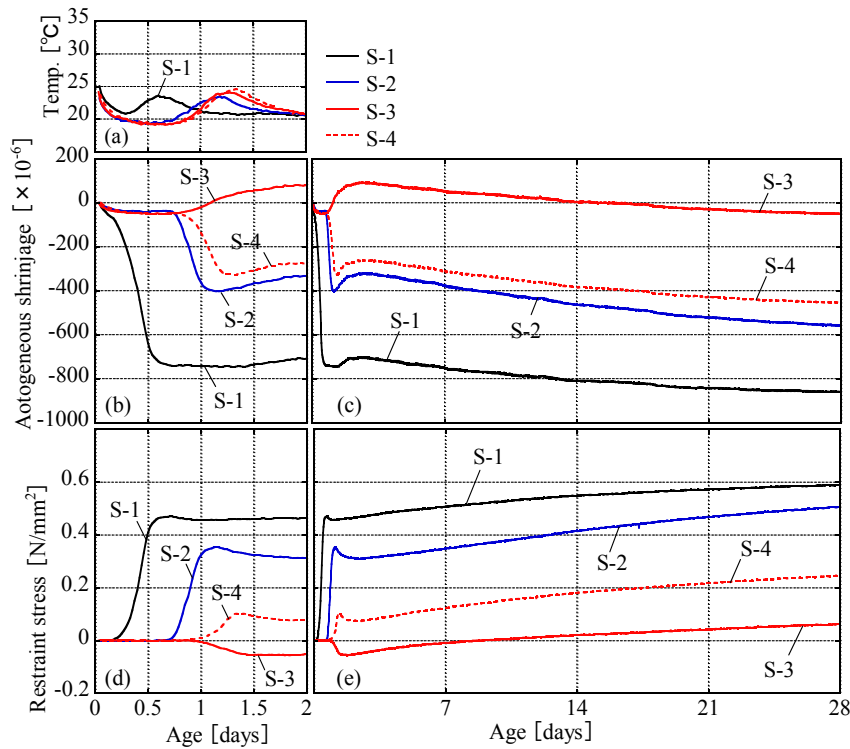


Fig. 8 – Autogenous shrinkage (series 2)

in Fig. 8(a), (b), and (d), shows the difference in their early behavior. The exotherm and shrinkage begin at the earliest time in S-1, followed by S-2, and then simultaneously by S-3 and S-4. Both the autogenous shrinkage strain and restraint stress are ranked as S-3 < S-4 < S-2 < S-1, with the autogenous shrinkage of S-3 being found to be extremely small. This is considered to be the “factor that determines the compressive strength of concrete other than the strength and stiffness of coarse aggregate and the mortar phase” mentioned in Section 2.2.2. Concretes of S3 mixtures are less prone to the risk of local stress fracture under compressive loading because of the low internal stress, which is generated by coarse aggregate restraining the autogenous shrinkage of the mortar phase.

One reason for the large autogenous shrinkage of S-1 is presumed to be the low elastic modulus of mortar, which is caused by lower stiffness of fine aggregate S1 than the others, leading to a lower degree of autogenous shrinkage restraint in the pastes. Another possibility is the effect of the shrinkage of fine aggregate itself (the shrinkage of S1 is greater than those of the other fine aggregates). These subject remains to be tackled in the future. Meanwhile, the autogenous shrinkage of S-3 is extremely small, though the elastic moduli of the mortars of S-3 and S-4 are similarly high. The differences between fine aggregates S3 and S4 include the large water absorption of S3 (S3: 2.91%, S4: 0.95%).

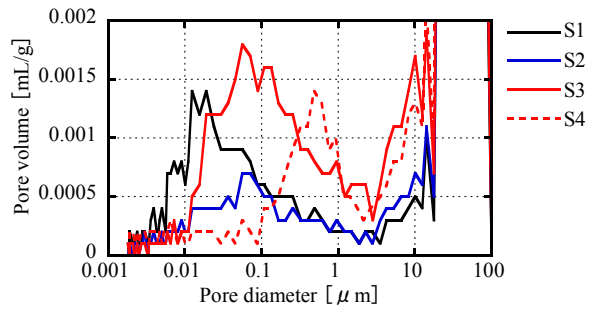


Fig. 9 – Pore size distribution of fine aggregate

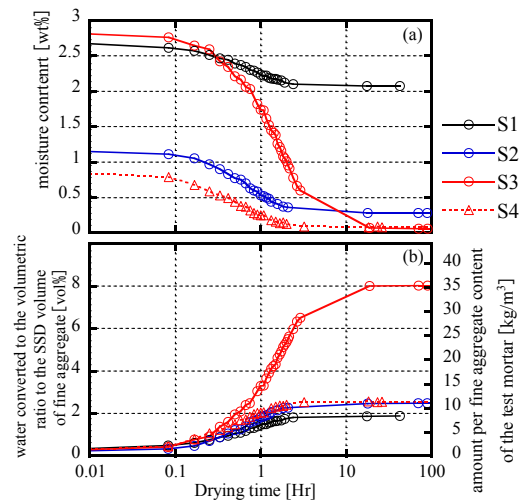


Fig. 10 – Changes in the moisture content of fine aggregates

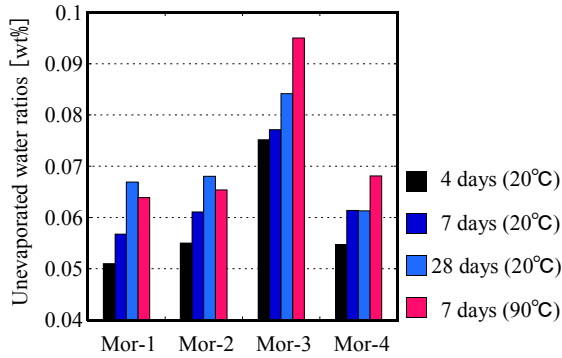


Fig. 11 – Unevaporated water ratios

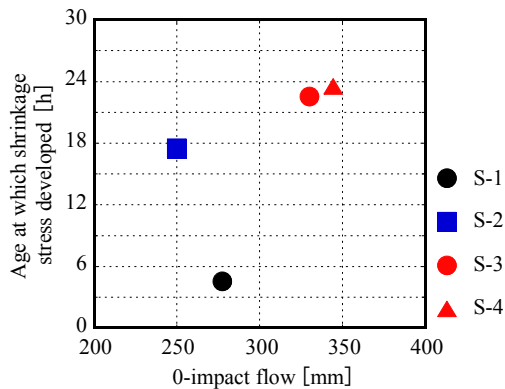


Fig. 12 – Relationship between the 0-impact flow and the age at which the shrinkage stress developed

It is therefore possible that the autogenous shrinkage of S-3 is reduced by the internal curing effect whereby the paste is supplied with water from fine aggregate [9].

### 3.2.4 Effects of fine aggregates on the mortar properties

Figure 9 shows the pore size distribution of fine aggregate. The peak pore size varies depending on the fine aggregate type, being  $S1 < S2 \approx S3 < S4$ . While the water absorptions of S1 and S3 are similarly large, the pore structure of S3 is coarser than that of S1, being easier to releasing water, bringing about a greater internal curing effect. Although, S2 and S4 are similarly or more prone to releasing water in terms of the peak pore size, but their internal curing effect is weaker presumably due to the low water absorption. To verify this hypothesis, a SSD sample of approximately 100 g of each fine aggregate was placed on a dish for monitoring the mass changes (changes in the moisture content) in an environment of 20°C and 60% R.H. (see Fig. 10 (a)). The moisture content of S3 decreases at a higher ratio than that of S1. The reduction nearly leveled off by 24 h later, but the ultimate value of S1 remains high at around 2% in contrast to S3 at nearly 0%. Figure 10 (b) shows the amount of evaporated

water converted to the volumetric ratio to the SSD volume of fine aggregate (on the vertical axis on the left) and the amount per fine aggregate content of the test mortar (on the right). This figure reveals that the water supply from S3 in the paste is evidently larger than those from the other aggregates.

Also, Figure 8 (d) shows the restraining stress of S-3 turning to the negative side, demonstrating that its autogenous shrinkage behavior is on the expansion side at early ages. This can be a phenomenon similar to the case reported in the literature [10] in which artificial lightweight fine aggregate used for ultrahigh strength concrete was found to expand.

Figure 11 shows the unevaporated water ratios of the fine aggregates, which is here defined as  $[\{(unit\ water\ content + amount\ of\ water\ absorption\ of\ fine\ aggregate)\} \div amount\ of\ the\ binder\ (B)] [wt\%]$  based on the results of the measurement of evaporated water in mortar samples. The values of S-3 are prominently large, presumably because water contained in S3 is supplied to the paste, contributing to hydration. This indirectly explains the above-mentioned discussion. Accordingly, the internal curing effect of S-3 not only reduces autogenous shrinkage but also increases strength and elastic modulus.

Figure 12 shows the relationship between the 0-impact flow and the age at which the shrinkage stress developed. The 0-impact flows of S-1 and S-2 are smaller than those of S-3 and S-4. To explain this, it is necessary to consider their physical aspects including the shape and grading of fine aggregate. On the other hand, the reason for the extremely early exotherm and shrinkage initiation can be attributed to the effect of the adsorption of SP by fine aggregate, as pointed out in a past study [11]. It can be considered that fine aggregate S1 in S-1 adsorbs a large amount of SP, and this weakens the cement-dispersing effect in mortar, reducing the mobility, while accelerating hydration. S1 and S4 with coarse pore structures, which are easier to release water, are less likely to adsorb SP.

Accordingly, it is presumed that, under proportioning conditions with a low unit water content and high fine aggregate content, the effects of competitive adsorption of water and a chemical admixture by the binder, hydrates, and fine aggregate on the mobility, mechanical properties, and shrinkage properties are significant. The results of our earlier report [2] shown in Fig. 1 explain the phenomenon in which an increase in the content of fine aggregate with a coarse and water-absorptive pore structure increases the internal curing effect. It is necessary from now on to confirm the behavior of water and a chemical admixture in fine aggregate.



#### 4. Conclusions

The following conclusions can be drawn in this study:

- (1) When a coarse pore-structured fine aggregate with a large water absorption was used for concrete with a water-binder ratio of 0.12, unit water content of 135 kg/m<sup>3</sup>, and sand-aggregate ratio of 55%, the mobility, strength, and elastic modulus of concrete increased, with its autogenous shrinkage becoming extremely low. This is considered to be due to the internal curing effect of fine aggregate.
- (2) One possible reason for the increased strength of concrete mentioned in (1) above is the reduced autogenous shrinkage of the mortar phase, which reduces the possibility of failure induced by local stress.
- (3) The internal curing effect of fine aggregate mentioned in (1) above presumably increases as the unit water content decreases and as the fine aggregate content increases.

#### Acknowledgment

The authors express their gratitude to the staff of Sika Ltd. and Taiheiyo Cement Corporation for providing test materials and cooperation in the experimental work. They are also grateful to Professor Manabu Kanematsu, as well as to Messrs. Taku Koyama and Yasuhiro Goto of Tokyo University of Science, for their cooperation.

#### References

1. Matsuda, T.; Honda, K.; Hasuo, K.; and Noguchi, T. (2014) "Study on Ultra-High-Strength Concrete Using Silica Fume and Fly Ash," Proceedings of the Japan Concrete Institute, 36 (1), pp. 1462-1467. (*in Japanese*)
2. Matsuda, T.; Hasuo, K.; Honda, K.; Takata, A.; Katsuro, N.; and Noguchi, T. (2014) "Study on Ultra-High-Strength Concrete Using Silica Fume and Fly Ash Part 2. Autogenous Shrinkage Reduction and Inspection Experiment by RC Column," Summaries of Technical Papers of Annual Meeting, Architectural Institute of Japan, pp. 111-112. (*in Japanese*)
3. Watanabe, S.; Kuroiwa, S.; Jinnai, H. and Namiki, S. (2005) "Study on Physical Properties of Coarse Aggregate which Affects Compressive Strength of High Strength Concrete," Journal of Structural and Construction Engineering (Transactions of AIJ) No. 588, pp. 21-27. (*in Japanese*)
4. Takagi, R.; Higo, Y.; and Yoshimoto, M. (2009) "Study of Coarse Aggregate Elasticity Coefficients is Affect High Strength Concrete Performance," Proceedings of the Japan Concrete Institute, 31(1), pp. 157-162. (*in Japanese*)
5. Sakuramoto, F.; Suzuki, K.; and Takei, K. (1990) "Experimental Study on Ultra High Strength Concrete Part3. Effect of Aggregate Properties on Concrete Strength," Summaries of Technical Papers of Annual Meeting, Architectural Institute of Japan, pp. 495-496. (*in Japanese*)
6. Watanabe, S.; Masuda, Y.; Jinnai, H.; Kuroiwa, S.; and Namiki, S. (2007) "Study on Stress and Strain of Mortar and Coarse Aggregate in High Strength Concrete Under Compressive Stress Condition." Journal of Structural and Construction Engineering (Transactions of AIJ) No. 616, pp. 25-32. (*in Japanese*)
7. Watanabe, S.; Kuroiwa, S.; Jinnai, H.; and Namiki, S. (2006) "Study on Compressive Strength of High Strength Concrete which Mixed Two Kinds of Crushed Stones," Journal of Structural and Construction Engineering (Transactions of AIJ) No. 600, pp. 9-15. (*in Japanese*)
8. Kano, Y.; Matsuda, T.; and Hasuo, K. (2013) "Study on Evaluation Method Ultra-High-Strength Concrete Autogenous Shrinkage Part 1. Experiment Summary and Effectiveness of Uni-Axial Restraint Stress Test," Summaries of Technical Papers of Annual Meeting, Architectural Institute of Japan, pp. 57-58. (*in Japanese*)
9. Sungchul, B.; Hayano, H.; Noguchi, T.; and Nagai, H. (2009) "Study on The Effectiveness of Autogenous Shrinkage Crack Reduction of Lightweight Aggregate," Proceedings of the Japan Concrete Institute, 31(1), pp. 565-570. (*in Japanese*)
10. Kuroiwa, S.; Jinnai, H.; Namiki, S.; and Nawa, T. (2014) "Mitigation of Autogenous Shrinkage of High-Strength Concrete using Pre-Wetted Artificial Lightweight Fine Aggregate," Journal of Structural and Construction Engineering (Transactions of AIJ, 79 (695), pp. 19-26. (*in Japanese*)
11. Nakamura, S. and Kobayashi, S. (1999) "Influence of Interaction between Sand and Superplasticizer on Fluidity of Concrete." Proceedings of the Japan Concrete Institute, 21

(2), pp. 181-186. (*in Japanese*)